

## Full Paper

# The constitutive presence of commensal bacteria contributes to the abundance of cecal IgG2b<sup>+</sup> B cells and the supply of serum IgG2b reactive to commensal bacteria in adult mice

Hiraku OKADA<sup>1</sup>, Masato TSUDA<sup>1\*</sup>, Natsuki KOJIMA<sup>1</sup>, Hirofumi WATANABE<sup>1</sup>, Gaku HARATA<sup>2</sup>, Kenji MIYAZAWA<sup>2</sup>, Daisuke KYOUI<sup>1</sup>, Satoshi HACHIMURA<sup>3</sup>, Yoshimasa TAKAHASHI<sup>4</sup>, Kyoko TAKAHASHI<sup>5</sup> and Akira HOSONO<sup>1\*</sup>

<sup>1</sup>Department of Food Science and Technology, College of Bioresource Sciences, Nihon University, 1866 Kameino, Fujisawa-shi, Kanagawa 252-0880, Japan

<sup>2</sup>Technical Research Laboratory, Takanashi Milk Products Co., Ltd., 5 Honjuku-cho, Asahi-ku Yokohama-shi, Kanagawa 241-0023, Japan

<sup>3</sup>Research Center for Food Safety, Graduate School of Agricultural and Life Sciences, The University of Tokyo, 1-1-1 Yayoi, Bunkyo-ku, Tokyo 113-8657, Japan

<sup>4</sup>Research Center for Drug and Vaccine Development, National Institute of Infectious Diseases, 1-23-1 Toyama, Shinjuku-ku, Tokyo 162-8640, Japan

<sup>5</sup>Department of Zoological Science, College of Bioresource Sciences, Nihon University, 1866 Kameino, Fujisawa-shi, Kanagawa 252-0880, Japan

Received July 27, 2024; Accepted November 10, 2024; Published online in J-STAGE November 27, 2024

Immunoglobulin (Ig) G isotypes in the sera of healthy mice and humans react to commensal bacteria. We previously reported that BALB/c mice with normal gut microbiota possessed abundant B cells that produced IgG2b reactive to commensal bacteria in cecal patches (CePs), indicating a potential source of a systemic pool of commensal bacteria-reactive IgG2b. Mice housed under germ-free conditions demonstrate the importance of the gut microbiota in driving cecal IgG2b responses. However, it is unclear whether the constitutive presence of the gut microbiota and specific bacterial taxa are important for IgG2b responses in adult mice. In this study, we showed that elimination of the gut microbiota by mixed antibiotic treatment in adult mice decreased the abundance of IgG2b<sup>+</sup> B cells, follicular helper T (T<sub>fh</sub>) cells in CePs, and the serum levels of commensal bacteria-reactive IgG2b. Reduced IgG2b responses have also been observed in mice with an altered gut microbiota following treatment with ampicillin or vancomycin. Changes in the diversity and composition of the cecal microbiota, particularly a decrease in *Lachnospiraceae*, *Muribaculaceae*, *Ruminococcaceae*, and *Bacteroidaceae* abundance at the family level, were observed in these mice. In addition, depletion of CD4<sup>+</sup> T cells by the injection of neutralizing antibodies in adult mice reduced IgG2b responses. Our results suggest that specific gut bacteria susceptible to ampicillin and vancomycin play roles in providing an abundance of T<sub>fh</sub> cells to help the generation of IgG2b<sup>+</sup> B cells in CePs in adult mice, which may contribute to the supply of systemic commensal bacteria-reactive IgG2b.

**Key words:** immunoglobulin (Ig) G2b, commensal bacteria-reactive IgG, cecal patches, follicular helper T cells, antibiotics

## INTRODUCTION

Immunoglobulin G (IgG) is the most predominant immunoglobulin in the serum of mammals. IgG consists of several subclasses (e.g., IgG1, IgG2, IgG3, and IgG4 in humans and IgG1, IgG2a (2c), IgG2b, and IgG3 in mice). IgG can bind

to specific antigens and protect against a variety of pathogenic bacterial and viral infections [1]. Notably, healthy mice and humans have serum IgG reactivity to commensal bacteria [2–4]. These antibodies seem to bind to a wide range of bacteria and protect the host from infection by the causative bacteria of gut infectious diseases, such as *Escherichia coli* and *Staphylococcus*

\*Corresponding authors. Masato Tsuda (E-mail: tsuda.masato@nihon-u.ac.jp); Akira Hosono (E-mail: hosono.akira@nihon-u.ac.jp) (Supplementary materials: refer to J-STAGE <https://www.jstage.jst.go.jp/browse/bmfh/list/-char/en>)

©2025 BMFH Press



This is an open-access article distributed under the terms of the Creative Commons Attribution Non-Commercial No Derivatives (by-nc-nd) License. (CC-BY-NC-ND 4.0: <https://creativecommons.org/licenses/by-nc-nd/4.0/>)

*aureus* [5, 6]. Commensal bacteria-reactive (CBR) IgG is delivered via breast milk to newborns, who cannot produce these antibodies due to their immature immune systems, thus protecting their intestinal tracts and whole bodies from intestinal pathogens [2, 5]. As mice age to approximately 6 to 8 weeks, they obtain the ability to make these antibodies by themselves [2]. A recent report suggested that the generation of memory B cells or long-lived plasma cells that produce CBR-IgG is induced by exposure to microbial antigens in the colon at the neonatal stage before weaning in mice with a C57BL/6J background [7]. However, whether and how these antibodies are induced and/or maintained in adult mice are not well understood.

Gut-associated lymphoid tissues (GALTs), composed of Peyer's patches (PPs), cecal patches (CePs), colonic patches, and isolated lymphoid follicles, are well known as the main inductive sites of the intestine for the production of antigen-specific IgA<sup>+</sup> B cells. Unlike systemic lymphoid organs, PPs constitutively possess a germinal center (GC) in which B cells actively proliferate and undergo class-switch recombination (CSR) and somatic hypermutations [8, 9]. The differentiation into IgA<sup>+</sup> B cells in the GCs of PPs is promoted with the help of follicular dendritic cells and follicular helper T (Tfh) cells [10, 11]. In particular, Tfh cells are essential for the formation and maintenance of GCs [12], and they contribute to IgA induction in PPs [13–15]. CePs, part of the GALTs of the large intestine, have also been reported to generate IgA<sup>+</sup> B cells [16]. Notably, we previously found that the CePs of adult BALB/c mice housed under conventional or specific-pathogen-free (SPF) conditions possess a high frequency of IgG2b<sup>+</sup> B cells rather than IgA<sup>+</sup> B cells, among other GALTs [17]. Furthermore, IgG2b produced by B cells derived from CePs in these mice exhibited reactivity to commensal bacteria. As CBR-IgG2b was detected in the sera of these mice, we predicted that CePs may be a potential source of CBR-IgG2b in the systemic circulation. In addition, we have shown that germ-free mice have few IgG2b<sup>+</sup> B cells and Tfh cells within poorly developed CePs, along with lower levels of CBR-IgG2b in the serum, suggesting the importance of the gut microbiota in the induction of antibody production. However, it is unclear whether the persistent presence of the gut microbiota and the type of gut bacteria are essential for CeP-mediated CBR-IgG2b production in adult mice.

In this study, we demonstrated that the abundance of IgG2b<sup>+</sup> B cells and Tfh cells in CePs decreased after treatment with a mixture of antibiotics (to eliminate the gut microbiota) and with a single antibiotic, either ampicillin or vancomycin (to alter the composition of the gut microbiota), in adult BALB/c mice, along with a reduction in the amount of CBR-IgG2b in the serum. In addition, we showed that the depletion of CD4<sup>+</sup> T cells in adult mice decreased these IgG2b responses. Our results indicate that intestinal bacteria, particularly those susceptible to ampicillin or vancomycin, play a role in the systemic supply of CBR-IgG2b in a CD4<sup>+</sup> T cell-dependent manner, providing protective immunity against systemic infection from possibly translocated intestinal bacteria.

## MATERIALS AND METHODS

### Mice

Female BALB/c mice (6 to 8 weeks old) were purchased from CLEA Japan (Tokyo, Japan) and kept under conventional

conditions in a room of maintained at a temperature of 23–25°C with 40–60% humidity and a 12 hr:12 hr light-dark cycle. The mice were fed an MF diet purchased from Oriental Yeast Co., Ltd. (Tokyo, Japan) and deionized sterile water *ad libitum*. All animal experiments were performed according to the guidelines of Nihon University for the care and use of laboratory animals after being reviewed and approved by the Nihon University Animal Care and Use Committee.

### Antibiotic treatment

Ampicillin and neomycin were purchased from Sigma-Aldrich (St. Louis, MO, USA). Vancomycin and metronidazole were purchased from NACALAI TESQUE (Kyoto, Japan). To set up the experimental condition termed 'elimination of the gut microbiota', a broad-spectrum cocktail of antibiotics (Abx-MIX) composed of 1 g/L ampicillin, 1 g/L neomycin, 0.5 g/L vancomycin, and 0.25 g/L metronidazole was administered to the mice via drinking water for 4 weeks. To check for the removal of intestinal microbiota, we estimated bacterial loads in stools by culture methods using EG agar for anaerobic bacteria and TS agar for aerobic bacteria. The mice before treatment with Abx-MIX and those in the control group had more than 10<sup>9</sup> of both aerobic and anaerobic bacteria in the feces. The mice treated with Abx-MIX for four weeks had markedly reduced numbers (less than 5 × 10<sup>3</sup>) of both aerobic and anaerobic bacteria in their feces.

To set up the experimental condition termed 'alteration of the gut microbiota', the mice were administered individual antibiotic agents separately.

### Depletion of CD4<sup>+</sup> T cells

Mice were treated with intraperitoneal injections of 150 µg of anti-mouse CD4 (clone GK1.5, Bio X Cell, Lebanon, NH, USA) or rat IgG2b isotype control (clone LTF-2, Bio X Cell) antibodies in 200 µL of sterile phosphate-buffered saline (PBS). Antibodies were administered on days 0, 3, 5, 7, 9, and 13. The mice were sacrificed on day 14. Depletion of CD4<sup>+</sup> cells was checked by flowcytometry. Less than 0.15% and 0.25% of CD4<sup>+</sup> cells were detected in CePs and the spleen, respectively, in anti-CD4-treated mice, whereas the percentages were about 20% in both tissues in untreated mice. The depletion of Tfh cells in CePs was also confirmed after treatment with the neutralizing antibody (less than 0.02%).

### Preparation of serum samples

Blood samples were collected from mice in each experiment. To prepare serum, blood samples were centrifuged at 3,000 rpm and 4°C for 10 min. These serum samples were stored at –30°C until use.

### Antibody detection by enzyme-linked immunosorbent assay

The concentration of antibody isotypes was determined using a sandwich enzyme-linked immunosorbent assay (ELISA). Briefly, a goat anti-mouse IgG F(ab')<sub>2</sub> fragment antibody (Sigma-Aldrich) was used as a capture antibody to measure all antibody isotypes. Alkaline-phosphatase-conjugated goat anti-mouse IgA, IgG1, IgG2b, and IgG3 (Southern Biotech, Birmingham, AL, USA) were used to detect antibodies in the collected samples. Color development was achieved by adding p-nitrophenyl phosphate (Fujifilm Wako Pure Chemical Corporation, Osaka, Japan) as a substrate.

The level of CBR antibodies was measured using an ELISA, as described previously [17]. Briefly, to prepare commensal bacteria, feces were collected from conventionally housed BALB/c mice, homogenized in sterile PBS to a concentration of 0.2 g/mL, and filtered through a 40 µm cell strainer. The preparations were then centrifuged at 1,000 rpm for 5 min to remove debris. The supernatant was collected and washed twice with PBS, heat-killed at 85°C for 1 hr, and then resuspended in 10 mL of 0.05 M carbonate-bicarbonate buffer (pH 9.6). One hundred microliters of these preparations was added to coat the wells of an ELISA plate instead of the capture antibody described above. The optical density was measured at 405 nm using a Multiskan GO microplate spectrophotometer (Thermo Fisher Scientific, Waltham, MA, USA).

### Cell preparation

Single cells were prepared from CePs as previously described [17]. Briefly, CePs were washed with RPMI 1640 medium (Nissui, Tokyo, Japan) supplemented with 50 U/mL penicillin, 50 µg/mL streptomycin, 2 mM L-glutamine, and 50 µM 2-mercaptoethanol; minced into small pieces; and incubated in RPMI 1640 medium containing 10% fetal calf serum (FCS; Biowest, Nuaille, France), 1 mg/mL collagenase D (Roche Diagnostics, Rotkreuz, Switzerland), and 20 µg/mL DNase I (Roche Diagnostics) for 50 min. The cell suspensions were filtered through a 70 µm cell strainer, washed, and resuspended in RPMI 1640 medium containing 10% FCS.

### Flow cytometry analysis

Freshly isolated cells were washed in staining buffer formulated with Dulbecco's modified Eagle's medium (Sigma-Aldrich) containing 1% bovine serum albumin (Sigma-Aldrich), 10 mM HEPES, 2 mM sodium pyruvate, 10<sup>-3</sup> mM EDTA, and 0.01% NaN<sub>3</sub>. Cells were blocked with an anti-CD16/CD32 antibody (clone 93, BioLegend, San Diego, CA, USA) for 15 min and incubated with the optimal concentration of biotinylated anti-IgG2b (clone R12-3, BD Biosciences, Franklin Lakes, NJ, USA), biotinylated anti-IgG1 (A85-1, BD Biosciences), biotinylated anti-IgG3 (R40-82, BD Biosciences), biotinylated anti-IgM (II/41, eBioscience, San Diego, CA, USA), biotinylated anti-IgA (11-44-2, eBioscience), biotinylated anti-CXCR5 (SPRCL5, eBioscience, San Diego, CA, USA), biotinylated rat IgG1 isotype control (eBRG1, eBioscience), biotinylated rat IgG2a isotype control (eBR2a, eBioscience), fluorescein isothiocyanate (FITC)-conjugated anti-CD4 (RM4-5, BioLegend), PerCPCyanin5.5-conjugated anti-mouse CD3ε (145-2C11, BioLegend), allophycocyanin (APC)-conjugated anti-programmed cell death protein 1 (PD-1) (RMP1-30, BioLegend), FITC-conjugated anti-B220 (RA3-6B2, BioLegend), phycoerythrin (PE)-conjugated anti-GL7 (GL-7, BD Biosciences), or Alexa Fluor 647-conjugated anti-CD95 (Jo2, BD Biosciences) antibodies; streptavidin-PE; or streptavidin PE-Cyanine7 (eBioscience) for 20 min on ice. The cells were then washed and resuspended in staining buffer. Flow cytometric analyses were performed using a FACS Canto instrument (BD Biosciences), and analyses were performed using FlowJo software v10.3 (Tree Star, Ashland, OR, USA).

### Analysis of the cecal microbiota

Bacterial DNA was extracted from the cecal contents using a NucleoSpin® DNA Stool kit (NS; MACHEREY-NAGEL GmbH & Co. KG, Düren, Germany). The concentration and quality of the purified DNA were analyzed using a Qubit fluorometer (Life Technologies, Carlsbad, CA, USA). To amplify the V3 and V4 regions of the bacterial 16S rRNA gene, polymerase chain reaction (PCR) was performed on a TaKaRa Cyclor Dice Touch (TaKaRa, Kusatsu, Japan) with 2× KAPA HiFi HotStart ReadyMix (Kapa Biosystems, Inc., Wilmington, MA, USA) under the following conditions: initial denaturation at 95°C for 3 min; followed by 25 cycles of 95°C for 30 sec, 55°C for 30 sec, and 72°C for 30 sec; and then a final extension step at 72°C for 5 min. The DNA concentration and size distribution of the prepared libraries were analyzed using a Qubit fluorometer and TapeStation instrument. The PCR products were purified using AMPure XP magnetic beads (Beckman Coulter Inc., Brea, CA, USA). Next, Illumina dual-index barcodes were added to the pooled PCR products using a Nextera XT Index Kit (Illumina, San Diego, CA, USA). Indexed PCR products were purified and pooled at equimolar concentrations prior to paired-end sequencing using MiSeq Reagent Kit v3 (600-cycle; Illumina) following the manufacturer's instructions. The QIIME II pipeline was used with the default parameters to identify representative sequences for amplicon sequence variants (ASVs) generated and aligned to the SILVA release 132 database [18, 19]. ASV tables with relative abundance percentages were processed at different taxonomic levels. Alpha and beta diversity calculations were performed and visualized using the QIIME script `core_diversity_analyses.py`. Beta-diversity calculations were visualized using principal coordinate analysis (PCoA) plots, based on the weighted UniFrac distance.

### Statistical analysis

Statistical significance was calculated using the IBM SPSS Statistics software (IBM SPSS Statistics 20, IBM Corp., Armonk, NY, USA). Data were analyzed using one-way analysis of variance, followed by Tukey's honestly significant difference (HSD) test or Dunnett's T3 test. An unpaired two-tailed Student's t-test was used to analyze the serum antibody concentrations. Differences were considered statistically significant at  $p < 0.05$ .

## RESULTS

### *Elimination of the gut microbiota by mixed antibiotic treatment decreased the abundance of IgG2b<sup>+</sup> B cells in CePs and the systemic circulation of commensal bacteria-reactive IgG2b in adult mice*

We previously showed that the number of IgG2b<sup>+</sup> B cells in CePs and the level of CBR-IgG2b in the serum decreased in germ-free mice, suggesting that the presence of the gut microbiota is important for the induction and/or maintenance of IgG2b production [17]. To examine whether the constitutive presence of the gut microbiota after birth is crucial for antibody production, adult BALB/c mice that had already developed a normal gut microbiota were administered a broad-spectrum cocktail of antibiotics (Abx-MIX) to eliminate most of the gut microbiota. First, we analyzed the concentrations of total IgG2b and CBR-IgG2b in the sera of the mice. Total IgG2b levels significantly

decreased in Abx-MIX-treated mice compared with control mice (Fig. 1a, left panel). Serum levels of CBR-IgG2b were also reduced in the Abx-MIX-treated mice (Fig. 1a, right panel). We measured the other isotypes of CBR antibodies in serum and found that CBR-IgG1 and CBR-IgG3 were also decreased in the Abx-MIX-treated mice (Supplementary Fig. 1).

Next, we analyzed IgG2b expression in the B cell populations of CePs. The proportion of IgG2b<sup>+</sup> B cells among the total B cell population in CePs was significantly decreased in Abx-MIX-treated mice (Fig. 1b). We then analyzed the population of IgG2b<sup>+</sup> B cells in terms of the GC reaction, because our previous study

showed that both GC and pre-GC B cells, but not naïve B cells, express high levels of IgG2b. The frequency and absolute number of GC (CD95<sup>+</sup>GL7<sup>+</sup>B220<sup>+</sup>) and pre-GC (CD95<sup>+</sup>GL7<sup>+</sup>B220<sup>+</sup>) B cells were lower in CePs from Abx-MIX-treated mice than in those from control mice (Fig. 1c and Supplementary Fig. 2a). In addition, although the expression level of IgG2b within GC and pre-GC B cells was not significantly decreased in CePs from Abx-MIX-treated mice than in those from control mice (Fig. 1d), the absolute numbers of IgG2b<sup>+</sup> GC B cells and IgG2b<sup>+</sup> pre-GC B cells were lower in CePs from Abx-MIX-treated mice than in those from control mice (Supplementary Fig. 2b). Furthermore,

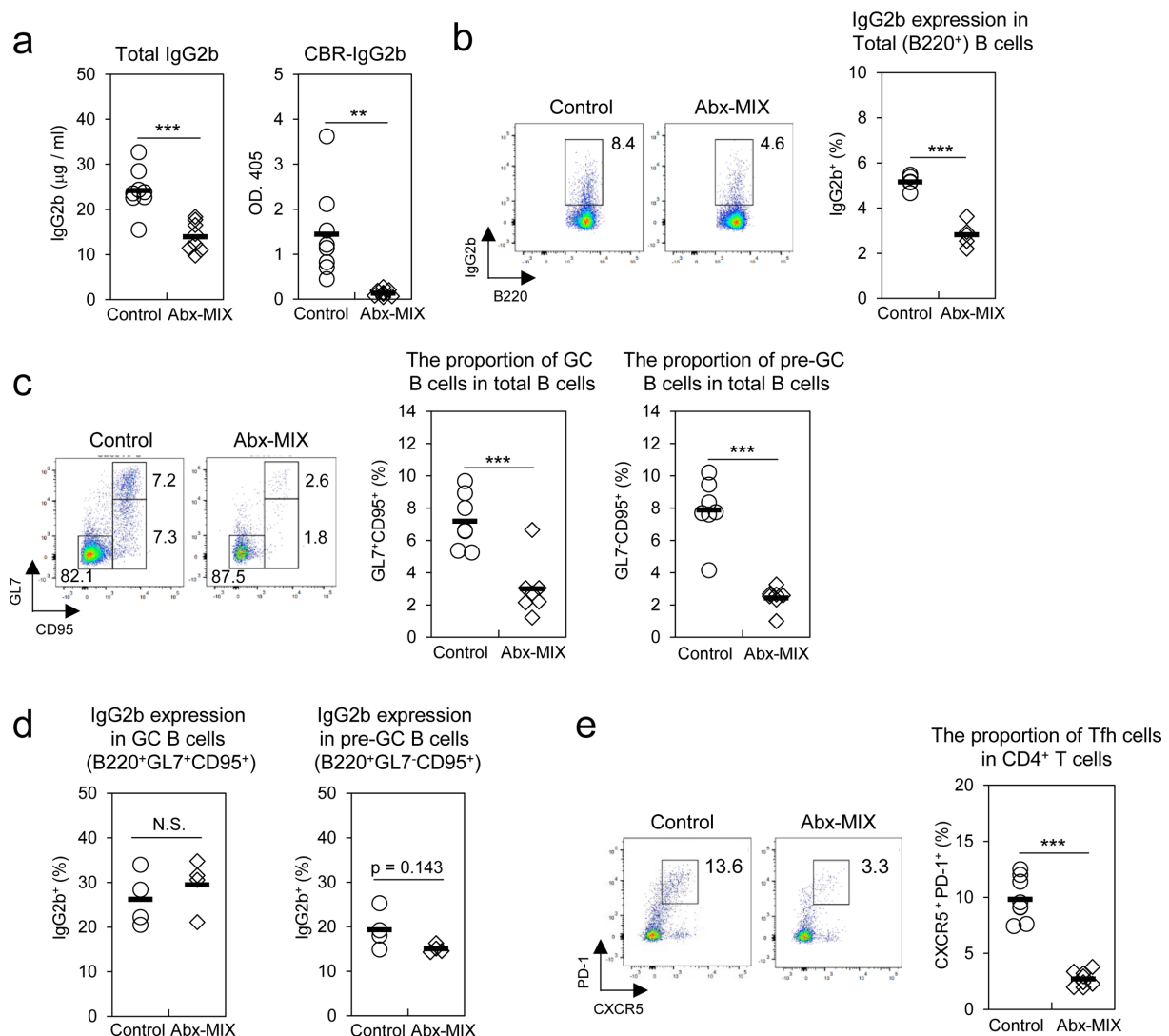


**Fig. 1.** Removal of the gut microbiota by treatment with Abx-MIX decreased CeP-derived IgG2b production and systemic commensal bacteria-reactive IgG2b in adult mice.

Adult BALB/c mice were treated with an antibiotic mixture (Abx-MIX) for 4 weeks. (a) Levels of total (left panel) and commensal bacteria-reactive (CBR)-IgG2b (right panel) in the serum. CBR-IgG2b titers are shown as net optical density at 405 nm (O.D. 405) units (the O.D. 405 of the blank was subtracted from the sample O.D. 405). Results are presented for six to eight individual animals in each group from a representative experiment. (b–e) Flow cytometric analysis of single cells of cecal patches (CePs) from control or Abx-MIX-treated mice. (b) Left panel: Flow cytometry dot plot of B220 and IgG2b expression gated to total B220<sup>+</sup> cells. Right panel: Percentage of IgG2b<sup>+</sup> cells among the total B cell population. (c) Left panel: Flow cytometry dot plot of CD95 and GL-7 expression in B220<sup>+</sup> B cells. Right panel: The percentage of germinal centers (GCs; CD95<sup>+</sup>GL7<sup>+</sup>B220<sup>+</sup>) and pre-GC (CD95<sup>+</sup>GL7<sup>+</sup>B220<sup>+</sup>) B cells among the total B cell population. (d) The percentage of the expression of IgG2b in GC and pre-GC B cells. (e) Left panel: Flow cytometry dot plot of CXCR5 and PD-1 expression gated on CD4<sup>+</sup> T cells. Right panel: Percentage of CXCR5<sup>+</sup>PD-1<sup>+</sup> Tfh cells. Representative flow cytometry dot plots are shown. Graphs of the flow cytometric analysis were obtained from at least five independent experiments. p-values were calculated using Student's t-test. \*p<0.05, \*\*p<0.01, \*\*\*p<0.001.



to understand the changes in the direction of class-switch recombination, we examined the expression of the other isotype of antibodies in each B cell fraction from CePs after Abx-MIX treatment. The expression of IgA and IgG1 in total B cells in CePs was decreased or tended to be decreased, respectively, after Abx-MIX treatment. In addition, the expression of IgA in GC and pre-GC B cells tended to be decreased, but the expression of IgG1 and IgG3 in GC and pre-GC B cells tended to be upregulated after Abx-MIX treatment (Supplementary Fig. 3). These results suggested that the reduction of IgG2b<sup>+</sup> B cells in CePs after Abx-MIX treatment was the result of a decrease in the number of GC and pre-GC B cells rather than the changes in the direction of class-switch recombination. Furthermore, we observed that the population of Tfh (CXCR5<sup>+</sup>PD-1<sup>+</sup>CD4<sup>+</sup>) cells was markedly decreased in CePs from Abx-MIX-treated mice (Fig. 1e). Taken together, these results suggested that the constant presence of the gut microbiota contributes to the abundance of IgG2b<sup>+</sup> B cells in CePs and the systemic pool of CBR-IgG2b.

#### ***Alteration of the gut microbiota by a single antibiotic treatment reduced the abundance of IgG2b<sup>+</sup> B cells in CePs and commensal bacteria-reactive IgG2b in the systemic circulation of adult mice***

Next, to understand the involvement of specific bacterial taxa that contribute to the induction/maintenance of IgG2b<sup>+</sup> B cells in CePs and CBR-IgG2b in the serum, mice were administered individual antibiotics (ampicillin, neomycin, metronidazole, and vancomycin) separately in drinking water. The total IgG2b concentrations in serum from both ampicillin- and vancomycin-treated mice were remarkably reduced compared with that of control mice (Fig. 2a, left panel). In addition, the level of CBR-IgG2b was significantly reduced in vancomycin-treated mice and tended to decrease in ampicillin-treated mice compared with control mice (Fig. 2a, right panel). The proportion of IgG2b<sup>+</sup> B cells among the total B cell population in CePs tended to decrease in both ampicillin- and vancomycin-treated mice (Fig. 2b). Following ampicillin treatment, the frequency of pre-GC B cells was decreased, and that of GC B cells showed a slight tendency to decrease (Fig. 2c). IgG2b expression in pre-GC B cells from CePs was reduced after ampicillin treatment (Fig. 2d). In addition, the proportion of Tfh cells in CePs tended to decrease in both ampicillin- and vancomycin-treated mice compared with control mice (Fig. 2e). Taken together, these results suggest that specific commensal bacteria susceptible to ampicillin and/or vancomycin may be involved in the cecal and systemic IgG2b responses.

#### ***Changes in the gut microbiota in adult mice after the administration of ampicillin and vancomycin***

To explore the involvement of specific commensal bacteria in CBR-IgG2b production, we analyzed the composition of the gut microbiota in the cecal contents of mice treated with antibiotics. Microbiota diversity, represented by Shannon and Chao-1 indices, was significantly reduced in ampicillin- and vancomycin-treated mice compared with other groups of mice (Fig. 3a). In addition, the relative abundances represented by the  $\beta$ -diversity of the cecal microbiota in the ampicillin- and vancomycin-treated mice were different from those of the control and other-antibiotic-treated mice (Fig. 3b). The dominant bacteria at the family level in the control group were *Lachnospiraceae* (45.30%), *Muribaculaceae* (20.25%), *Ruminococcaceae* (9.60%), and *Bacteroidaceae*

(7.50%). However, the abundances of these bacterial families were significantly reduced after treatment with ampicillin and/or vancomycin (Fig. 3c, 3d). These results suggested that ampicillin and/or vancomycin treatment reduced the abundances of specific gut bacteria potentially related to cecal and systemic IgG2b production.

#### ***The presence of CD4<sup>+</sup> T cells was important for the abundance of IgG2b<sup>+</sup> B cells in the CePs and commensal bacteria-reactive IgG2b in the serum of adult mice***

As shown in Figs. 1 and 2, treatment with Abx-MIX, ampicillin, or vancomycin decreased the systemic pool of IgG2b and the proportion of IgG2b<sup>+</sup> B cells in CePs, and this was accompanied by a reduction of Tfh cells in CePs. Therefore, we hypothesized that the induction and/or maintenance of Tfh cells in CePs by the constitutive presence of the gut microbiota is important for the generation of cecal IgG2b<sup>+</sup> B cells and the supply of systemic CBR-IgG2b. We investigated mice with depletion of CD4<sup>+</sup> T cells by intraperitoneal injection of a neutralizing antibody. After treatment, we checked the depletion of Tfh cells along with CD4<sup>+</sup> T cells in CePs as well as CD4<sup>+</sup> T cells in the spleen (see also MATERIALS AND METHODS). The level of total IgG2b in the serum was lower in CD4<sup>+</sup> T cell-depleted mice than in control mice (Fig. 4a). Furthermore, we detected CBR-IgG2b in the serum of control mice, and the antibody levels in these mice tended to decrease after the depletion of CD4<sup>+</sup> T cells (Fig. 4b). Next, we observed that CD4<sup>+</sup> T cell-depleted mice had a decreased frequency of IgG2b<sup>+</sup> B cells in CePs (Fig. 4c). In addition, compared with control mice, the frequency of GC B cells was lower in the CePs of CD4<sup>+</sup> T cell-depleted mice, and that of pre-GC B cells tended to be lower (Fig. 4d). The proportion of IgG2b<sup>+</sup> B cells among the GC and pre-GC B cell population was not significantly decreased in the CePs of CD4<sup>+</sup> T cell-depleted mice (Fig. 4e). Taken together, these results suggested that CD4<sup>+</sup> T cells, such as Tfh cells, play critical roles in generating IgG2b<sup>+</sup> B cells in CePs and in maintaining the systemic pool of CBR-IgG2b.

## **DISCUSSION**

Previous studies have shown that several antibody isotypes, i.e., IgA, IgM, IgG1, IgG2b, IgG2c, and IgG3, in the serum of mice have the ability to bind to gut microbiota [2, 3]. Among the IgG subclasses, IgG2b and IgG3 seem to have strong abilities to bind. These studies and our previous study have also demonstrated that gut microbiota have important roles in inducing these antibodies, as shown by the decrease in them in germ-free mice [2, 3, 17]. However, the mechanism underlying the induction and/or maintenance of commensal bacteria-reactive IgG (CBR-IgG) in the serum of adult mice remains unclear. We focused on the cellular responses of CePs, which are a part of the GALTs located in the cecum, to generate abundant IgG2b<sup>+</sup> B cells. Our previous study reported that BALB/c mice housed under germ-free conditions have fewer IgG2b<sup>+</sup> B cells and Tfh cells in CePs and lower levels of CBR-IgG2b in the blood than mice housed under conventional conditions [17]. The present study showed that the population of IgG2b<sup>+</sup> B cells in CePs and the levels of CBR-IgG2b in the systemic circulation decreased in adult mice when their gut microbiota were eliminated by treatment with Abx-Mix for 4 weeks. Therefore, these results suggested that the generation

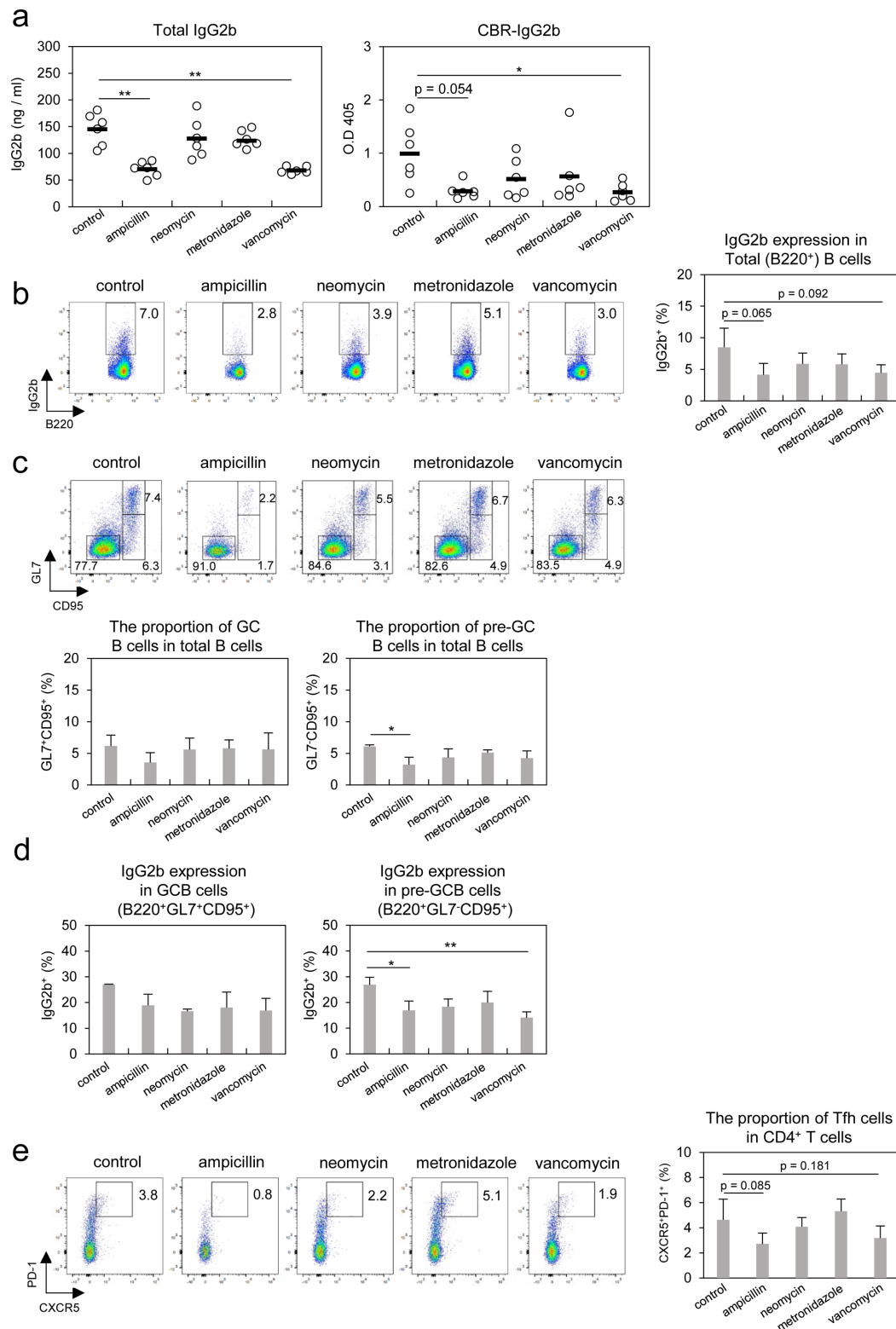


**Fig. 2.** Individual antibiotic treatment affected the abundance of IgG2b<sup>+</sup> B cells in CePs and systemic commensal bacteria-reactive IgG2b.

Adult BALB/c mice were individually treated with antibiotics for 4 weeks. (a) Levels of total IgG2b (left panel) and CBR-IgG2b (right panel) in the serum. CBR-IgG2b titers are shown as net O.D. 405 units (the O.D. 405 of the blank was subtracted from the sample O.D. 405). Results are presented for five animals in each group from a representative experiment. (b–e) Flow cytometric analysis of single cells of pooled CePs from each group of antibiotic-treated mice. (b) Left panel: Flow cytometry dot plot of IgG2b antibody expression gated to B220<sup>+</sup> B cells. Right panel: Percentage of IgG2b<sup>+</sup> cells among the total B cell population. (c) Upper panel: CD95 and GL-7 expression gated to B220<sup>+</sup> B cells. Lower panel: Percentage of GC and pre-GC B cells among the total B cell population. (d) The percentage of IgG2b expression in GC and pre-GC B cells of CePs. (e) Left panel: CXCR5 and PD-1 expression gated to CD4<sup>+</sup> T cells. Right panel: Percentage of CXCR5<sup>+</sup>PD-1<sup>+</sup> Tfh cells. Representative flow cytometry dot plots are shown. Data are presented as the mean  $\pm$  standard deviation (S.D.) from four independent experiments. p-values were calculated using a one-way analysis of variance (ANOVA) followed by Tukey's HSD test or Dunnett's T3 test (b–e). \*p < 0.05, \*\*p < 0.01, \*\*\*p < 0.001.

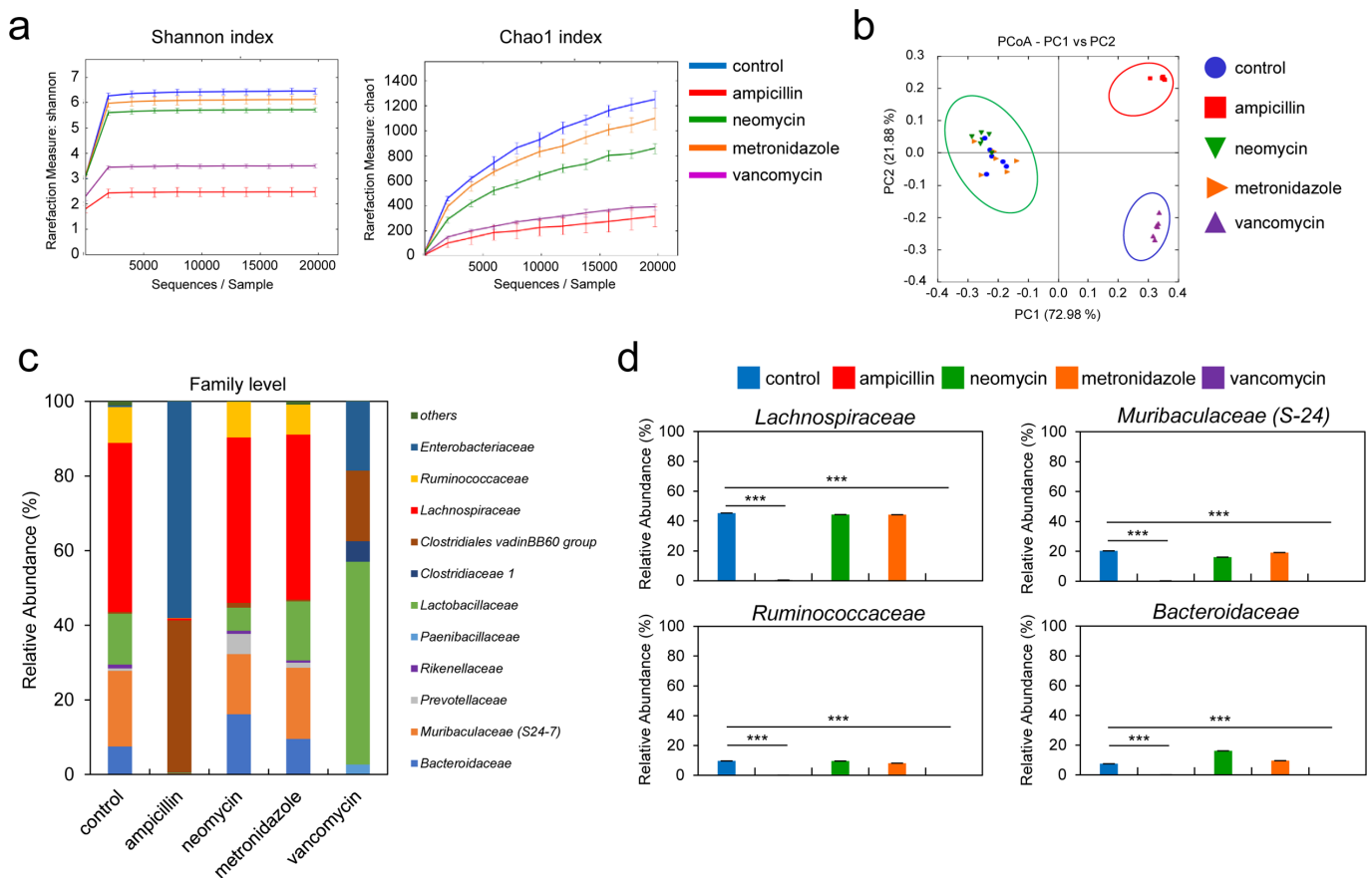


**Fig. 3.** Alteration of the composition and diversity of the cecal microbiota after individual antibiotic treatment.

16S rRNA gene analysis was performed on DNA extracted from the cecal contents of mice treated with individual antibiotics after 4 weeks. (a) Alpha diversity analysis of the cecal microbiota. Alpha diversity analysis assessed the species diversity within a single sample and included the observed Shannon index (left panel) and the Chao index (right panel). (b) Beta diversity analysis of the cecal microbiota. (c) Abundance distribution map at the family level. The horizontal axis represents the sample name, and the vertical axis represents the relative abundance of annotated species. (d) Relative abundance of specific bacterial families. Data were obtained from six individual mice from each group and are shown as the mean  $\pm$  SD. p-values were calculated using one-way ANOVA followed by Tukey's HSD test or Dunnett's T3 test. \* $p < 0.05$ , \*\* $p < 0.01$ , \*\*\* $p < 0.001$ . See also the analysis of the cecal microbiota in the Materials and Methods section.

of IgG2b<sup>+</sup> B cells in CePs and the supply of CBR-IgG2b in the blood require the constitutive presence of the gut microbiota in adult mice. Mechanistically, we speculated that the relatively short-lived plasma cell pool producing CBR-IgG2b induced from CePs was diminished by continuous Abx-MIX-treatment in adult mice.

The mice treated with ampicillin or vancomycin showed a similar decrease in IgG2b antibody responses to that with Abx-MIX. The abundance of bacterial families, such as *Lachnospiraceae*, *Muribaculaceae*, *Ruminococcaceae*, and *Bacteroidaceae*, decreased after the administration of either ampicillin or vancomycin. Hence, these results indicated the possible roles of these bacterial families in the production of CBR-IgG2b. A previous report showed that GC formation in CePs was facilitated by the association of a single gram-negative bacterium, *Bacteroides acidifaciens*, belonging to *Bacteroidaceae* in germ-free mice [20]. As GC B cells in CePs expressed high levels of IgG2b, the reduction in the number of IgG2b<sup>+</sup> B cells, along with GC B cells, in CePs in antibiotic-treated mice might have been caused by a reduction in *Bacteroidaceae*. Furthermore, *Lachnospiraceae* and *Ruminococcaceae* are generally classified

as butyrate-producing bacteria, indicating a potential role for short-chain fatty acids in antibody responses. Indeed, a study using *in vitro* culture systems showed that stimulation with butyrate enhances the differentiation of naïve B cells into B cells expressing IgG isotypes, including IgG2b, by modulating energy metabolism [21].

It remains unknown which microbial components or metabolites are more important for inducing IgG2b responses. Koch *et al.* reported that signaling through TLR2 and TLR4 in B cells is required to drive the differentiation of naïve B cells into plasma cells that produce IgG2b and IgG3, resulting in CBR-IgG2b and CBR-IgG3 [2]. More recent studies have shown that muramyl dipeptide, an agonist of Nod2, which is a type of Nod-like receptor that plays an important role in microbiota-dependent signaling, can promote IgG2b switching in mouse B cells via activation of TLR4 by co-stimulation with lipopolysaccharide [22]. In line with these reports, we demonstrated that myeloid differentiation factor 88 (MyD88) knockout mice housed under SPF conditions reduced the abundance of IgG2b<sup>+</sup> B cells in CePs and the levels of CBR-IgG2b in the blood [17]. This evidence indicates that stimulation/signaling by microbial components

(i.e., cell wall components and/or nucleic acids) through pattern recognition receptors in specific gut bacteria is important for the generation of IgG2b<sup>+</sup> B cells in CePs and the supply of CBR-IgG2b to the systemic circulation.

In the present study, we observed that the reduction in the number of IgG2b<sup>+</sup> B cells in CePs after treatment with a mixture of antibiotics and/or a single antibiotic agent in adult BALB/c mice housed under conventional conditions was accompanied by a reduction in the number of Tfh cells. In addition, the depletion

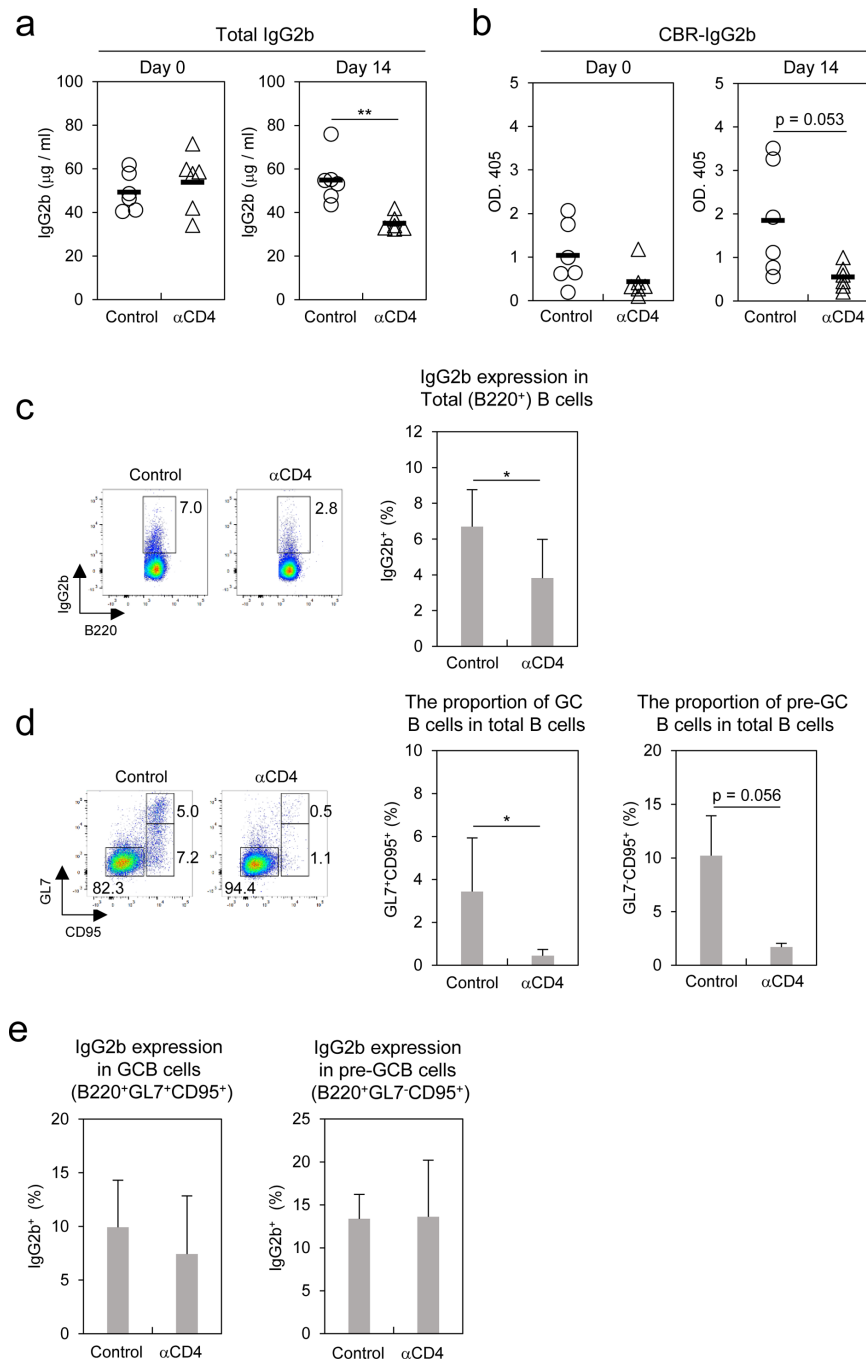


**Fig. 4.** Involvement of CD4<sup>+</sup> T cells in commensal bacteria-reactive IgG2b in the systemic circulation, and IgG2b<sup>+</sup> B cells in CePs.

Adult BALB/c mice were intraperitoneally administered an anti-CD4 neutralizing antibody or an isotype control antibody six times within 2 weeks. (a–b) Levels of total IgG2b (a) and CBR-IgG2b (b) on days 0 and 14. The levels of CBR-IgG2b are shown as net O.D. 405 units (the O.D. 405 of the blank was subtracted from the sample O.D. 405). Results are presented for six animals in each group from at least three independent experiments. (c–e) Flow cytometry analysis of single cells of pooled CePs from each group. (c) Left panel: Flow cytometric dot plot of B220 and IgG2b expression gated on B220<sup>+</sup> B cells. Right panel: Percentage of IgG2b<sup>+</sup> cells among the total B cell population. (d) Left panel: Flow cytometry dot plot of CD95 and GL-7 expression gated on B220<sup>+</sup> B cells. Right panel: Percentage of GC and pre-GC B cells among the total B cell population. (e) The percentage of GC and pre-GC B cells expressing IgG2b in CePs. Representative flow cytometry dot plots are shown for at least three independent experiments. p-values were calculated using Student's t-tests. \*p<0.05, \*\*p<0.01, \*\*\*p<0.001.



of CD4<sup>+</sup> T cells in adult mice also reduced the abundance of IgG2b<sup>+</sup> B cells in CePs, as well as the level of IgG2b in the serum. Thus, it is possible that CD4<sup>+</sup> T cells, including Tfh cells, in CePs are responsible for gut-microbiota-mediated IgG2b production. Generally, antibody responses mediated by MyD88 signaling through pattern recognition receptors are induced in a T cell-independent manner. Of note, it has been reported that CD4<sup>+</sup> T cell-intrinsic MyD88 signaling is important for the development of Tfh cells in PPs that direct GC B cells and antigen-specific IgA against the microbiota [23]. Considering these points, it is possible that gut-microbiota-induced MyD88 signaling within CD4<sup>+</sup> T cells may be responsible for the development of Tfh cells and the induction of IgG2b<sup>+</sup> B cells in CePs, contributing to the systemic supply of CBR-IgG2b.

Collectively, our data demonstrate that the constitutive presence of members of the gut microbiota that are susceptible to ampicillin and vancomycin is important for the generation of IgG2b<sup>+</sup> B cells in CePs and the supply of systemic CBR-IgG2b via the existence of CD4<sup>+</sup> T cells, such as Tfh cells, in normally raised adult mice. Although the function of systemic CBR-IgG2b is still largely unknown, a previous report has shown that systemic IgG (particularly IgG2b subclass) reactive to commensal bacteria binds to murein lipoprotein, a highly conserved outer membrane protein expressed abundantly in gram-negative bacteria, and plays a role in protecting against opportunistic pathogenic bacteria, such as gram-negative *E. coli* and *Klebsiella pneumoniae*, in healthy adult mice [3]. Therefore, methods to control the ability of candidate bacteria to modulate cecal IgG2b production will prevent infections and inflammatory diseases caused by the translocation of intestinal bacteria into the systemic circulation. Further studies are required to evaluate the precise function of CeP-mediated CBR-IgG2b production.

## FUNDING

This study was supported by grants from the Japan Society for the Promotion of Science (KAKENHI 15K07443 to A.H. and 17K15277 and 20K05914 to M.T.).

## CONFLICTS OF INTEREST

The authors have no conflicts of interest to declare.

## REFERENCES

- Collins AM. 2016. IgG subclass co-expression brings harmony to the quartet model of murine IgG function. *Immunol Cell Biol* 94: 949–954. [Medline] [CrossRef]
- Koch MA, Reiner GL, Lugo KA, Kreuk LS, Stanbery AG, Ansaldo E, Seher TD, Ludington WB, Barton GM. 2016. Maternal IgG and IgA antibodies dampen mucosal T helper cell responses in early life. *Cell* 165: 827–841. [Medline] [CrossRef]
- Zeng MY, Cisalpino D, Varadarajan S, Hellman J, Warren HS, Cascalho M, Inohara N, Núñez G. 2016. Gut microbiota-induced immunoglobulin G controls systemic infection by symbiotic bacteria and pathogens. *Immunity* 44: 647–658. [Medline] [CrossRef]
- Fadlallah J, Sterlin D, Fieschi C, Parizot C, Dorgham K, El Kafsi H, Autaa G, Ghillani-Dalbin P, Juste C, Lepage P, et al. 2019. Synergistic convergence of microbiota-specific systemic IgG and secretory IgA. *J Allergy Clin Immunol* 143: 1575–1585.e4. [Medline] [CrossRef]
- Zheng W, Zhao W, Wu M, Song X, Caro F, Sun X, Gazzaniga F, Stefanetti G, Oh S, Mekalanos JJ, et al. 2020. Microbiota-targeted maternal antibodies protect neonates from enteric infection. *Nature* 577: 543–548. [Medline] [CrossRef]
- Chen X, Gula H, Pius T, Ou C, Gomozkova M, Wang LX, Schneewind O, Missiakas D. 2023. Immunoglobulin G subclasses confer protection against *Staphylococcus aureus* bloodstream dissemination through distinct mechanisms in mouse models. *Proc Natl Acad Sci USA* 120: e2220765120. [Medline] [CrossRef]
- Rusconi B, Bard AK, McDonough R, Kindsvogel AM, Wang JD, Udayan S, McDonald KG, Newberry RD, Tarr PI. 2024. Intergenerational protective anti-gut commensal immunoglobulin G originates in early life. *Proc Natl Acad Sci USA* 121: e2309994121. [Medline] [CrossRef]
- Cerutti A. 2008. The regulation of IgA class switching. *Nat Rev Immunol* 8: 421–434. [Medline] [CrossRef]
- Suzuki K, Kawamoto S, Maruya M, Fagarasan S. 2010. GALT: organization and dynamics leading to IgA synthesis. *Adv Immunol* 107: 153–185. [Medline] [CrossRef]
- Beller A, Kruglov A, Durek P, von Goetze V, Werner K, Heinz GA, Ninnemann J, Lehmann K, Maier R, Hoffmann U, et al. 2020. Specific microbiota enhances intestinal IgA levels by inducing TGF- $\beta$  in T follicular helper cells of Peyer's patches in mice. *Eur J Immunol* 50: 783–794. [Medline] [CrossRef]
- Hashiguchi M, Kashiwakura Y, Kanno Y, Kojima H, Kobata T. 2020. IL-21 and IL-5 coordinately induce surface IgA<sup>+</sup> cells. *Immunol Lett* 224: 21–27. [Medline] [CrossRef]
- Crotty S. 2011. Follicular helper CD4 T cells (TFH). *Annu Rev Immunol* 29: 621–663. [Medline] [CrossRef]
- Tsuji M, Komatsu N, Kawamoto S, Suzuki K, Kanagawa O, Honjo T, Hori S, Fagarasan S. 2009. Preferential generation of follicular B helper T cells from Foxp3<sup>+</sup> T cells in gut Peyer's patches. *Science* 323: 1488–1492. [Medline] [CrossRef]
- Hirota K, Turner JE, Villa M, Duarte JH, Demengeot J, Steinmetz OM, Stockinger B. 2013. Plasticity of Th17 cells in Peyer's patches is responsible for the induction of T cell-dependent IgA responses. *Nat Immunol* 14: 372–379. [Medline] [CrossRef]
- Kato LM, Kawamoto S, Maruya M, Fagarasan S. 2014. Gut TFH and IgA: key players for regulation of bacterial communities and immune homeostasis. *Immunol Cell Biol* 92: 49–56. [Medline] [CrossRef]
- Masahata K, Umamoto E, Kayama H, Kotani M, Nakamura S, Kurakawa T, Kikuta J, Gotoh K, Motooka D, Sato S, et al. 2014. Generation of colonic IgA-secreting cells in the caecal patch. *Nat Commun* 5: 3704. [Medline] [CrossRef]
- Tsuda M, Okada H, Kojima N, Ishihama F, Muraki Y, Oguma T, Hattori N, Mizoguchi T, Mori K, Hachimura S, et al. 2022. Cecal patches generate abundant IgG2b-bearing B cells that are reactive to commensal microbiota. *J Immunol Res* 2022: 3974141. [Medline] [CrossRef]
- Bolyen E, Rideout JR, Dillon MR, Bokulich NA, Abnet CC, Al-Ghalith GA, Alexander H, Alm EJ, Arumugam M, Asnicar F, et al. 2019. Reproducible, interactive, scalable and extensible microbiome data science using QIIME 2. *Nat Biotechnol* 37: 852–857. [Medline] [CrossRef]
- Quast C, Pruesse E, Yilmaz P, Gerken J, Schweer T, Yarza P, Peplies J, Glöckner FO. 2013. The SILVA ribosomal RNA gene database project: improved data processing and web-based tools. *Nucleic Acids Res* 41: D590–D596. [Medline] [CrossRef]
- Yanagibashi T, Hosono A, Oyama A, Tsuda M, Suzuki A, Hachimura S, Takahashi Y, Momose Y, Itoh K, Hirayama K, et al. 2013. IgA production in the large intestine is modulated by a different mechanism than in the small intestine: bacteroides acidifaciens promotes IgA production in the large intestine by inducing germinal center formation and increasing the number of IgA<sup>+</sup> B cells. *Immunobiology* 218: 645–651. [Medline] [CrossRef]
- Kim M, Qie Y, Park J, Kim CH. 2016. Gut microbial metabolites fuel host antibody responses. *Cell Host Microbe* 20: 202–214. [Medline] [CrossRef]
- Lee SH, Park JH, Park SR. 2019. The Nod2 agonist muramyl dipeptide cooperates with the TLR4 agonist lipopolysaccharide to enhance IgG2b production in mouse B cells. *J Immunol Res* 2019: 2724078. [Medline] [CrossRef]
- Kubinak JL, Petersen C, Stephens WZ, Soto R, Bake E, O'Connell RM, Round JL. 2015. MyD88 signaling in T cells directs IgA-mediated control of the microbiota to promote health. *Cell Host Microbe* 17: 153–163. [Medline] [CrossRef]